

TRANSMISSION ELECTRON MICROSCOPY STUDY OF THIN FILMS AND SURFACE IMPLANTED WAFERS OF LiNbO_3

V.S. Teodorescu, C. Ghica, M.G. Blanchin^a, P. Moretti^b

National Institute for Physics of Materials, P.O.Box Mg. 7, 76900 - Bucharest, Romania
^aDépartement de Physique des Matériaux, CNRS UMR 5586, Université Claude Bernard,
69622 Villeurbanne Cedex, France

^bLaboratoire de Physico-Chimie des Matériaux Luminescents, CNRS UMR 5620, Université
Claude Bernard, 69622 Villeurbanne Cedex, France

Thin films prepared by pulsed laser deposition and single crystal implanted LiNbO_3 wafers used in optoelectronic technology were studied by transmission electron microscopy. The use of high electron beam density for high resolution imaging induced a decomposition effect in the implanted LiNbO_3 lattice. It is shown that the most probable decomposition leads to the formation of NbO_2 nuclei by a topotactic solid state reaction along the pseudo-cubic directions of the lithium niobate matrix. It is also shown that powdered LiNbO_3 specimens or samples obtained by preparation of cross section of LiNbO_3 thin films are more stable in the electron beam, compared with the samples obtained from implanted LiNbO_3 wafers.

(Received June, 4, 1999; accepted June 18, 1999)

Keywords: Electron microscopy, LiNbO_3 , Radiation damage

1. Introduction

Lithium niobate (LiNbO_3) is nowadays one of the most used electro-optic material due to its outstanding physical properties [1,2]. LiNbO_3 single crystal wafers and also LiNbO_3 thin films grown by different methods [3-5] are often involved in optoelectronics and microscopic studies are widely used for structural investigations. In the last time, the new techniques developed for cross section observation by transmission electron microscopy are involved more and more in the study of the structural features of the lithium niobate applied in various microsystems.

Like many oxides and all ionic crystals [6,7], LiNbO_3 is sensitive to the intense electron beam used in transmission electron microscopy (TEM). This sensitivity depends of the sample stoichiometry and sample preparation technique. Our TEM study on thin foils of erbium implanted LiNbO_3 crystals [8,9] shows a structural modification of the crystal lattice under the electron beam, during microscopic observation. However, in the case of similar observations on samples prepared by classical way of powder deposited on holey carbon grids for high resolution, such modifications does not appear [10]. The same good stability is observed in the case of thin film observation [5].

In this paper we show some of the structural aspects which can be observed using TEM and the associated selected area electron diffraction (SAED) investigations and we point out the effects of electron irradiation damage in LiNbO_3 structure observed with a 200 kV microscope under the usual conditions for diffraction and imaging at increasing magnifications.

2. Experimental

The preparation of the samples for TEM observation depends, generally, upon the structural information that has to be expected from such a study. When structural and compositional studies are needed, the simple grinding of the LiNbO_3 crystal and a holey carbon grid preparation are enough for carrying out observations in the microscope. In such cases, high resolution images on various crystal orientations can be obtained, but the morphology of the overall sample is lost. Nevertheless, the morphology of the nanoscale structure of the defects and other features is conserved and can be successfully studied.

In the case of thin films or surface structures the most important aspect to be visualized is the cross section structure and several techniques can be applied to this purpose. Generally, the samples are glued face to face and after a properly mechanical cutting and polishing, finally ionic thinning is used for the TEM specimen production [5].

Thin foils in cross section geometry were prepared also by the same ion thinning method starting from Er implanted commercially available LiNbO_3 single crystals. In the geometry of this preparation, the viewing zone axis of the TEM observations is $[1\bar{1}20]$ [8]. The thin foils were observed directly in the electron beam, without carbon average. No charge accumulation was noted, but some structural modifications occur during TEM observations at high magnifications. Even at the minimum current density (20-30 A/cm^2) required for recording high (spatial) resolution image, the contrast in the observed area do change after several minutes of observation.

TEM images have been obtained in the Jeol 200 CX and Topcon 002B electron microscopes.

3. Results and discussion

3.1. Thin film observations

The cross section studies by TEM provides the most useful structural information on the films. Fig. 1 shows two sections of two different LiNbO_3 thin films obtained by pulsed laser deposition from a LiNbO_3 target in residual oxygen atmosphere [5].

The films are deposited on Si substrates and their structure are different because of the deposition conditions and the after deposition thermal treatment. First film is deposited at low (500°C) substrate temperature and show crystallites smaller than 30 nm an average and a quite good uniformity. This film shows a lot of small voids which can be easy observed in Fig. 1a. Such voids are generally not convenient for optoelectronic applications. However, the higher temperature deposition and the post deposition thermal treatment lead to the appearance of a columnar morphology with crystallites of about 100 to 200 nm in diameter. In this case, no voids are present and the density of the LiNbO_3 film is close to the bulk value. However, the columnar morphology with the (0001) texture introduces an anisotropy effect, which can be a shortcoming for some applications.

3.2. Implanted LiNbO_3 wafers

One of the wave-guide technologies uses the surface implantation of LiNbO_3 wafers. In this case it is important to observe the implanted layer and to find out the structural state of this layer. Fig. 2a shows a TEM image of such a surface layer obtain by erbium ion implantation. No dislocations or other extended defects can be observed at the implanted surface [9].

Implantation of heavy ions like Er (here 2×10^{16} ions/ cm^2 at 300 keV) induces true amorphisation and also generates surface sputtering which may include preferential loss of O and Li [1]. After implantation the crystals are annealed at 1100 °C for 20 h so that the LiNbO_3 lattice is restored without extended defects. This restoration does occur by diffusion of the atomic species over large distances in the bulk and probably lead to the formation of a non-stoichiometric layer over several micrometers below the surface of the LiNbO_3 wafer.

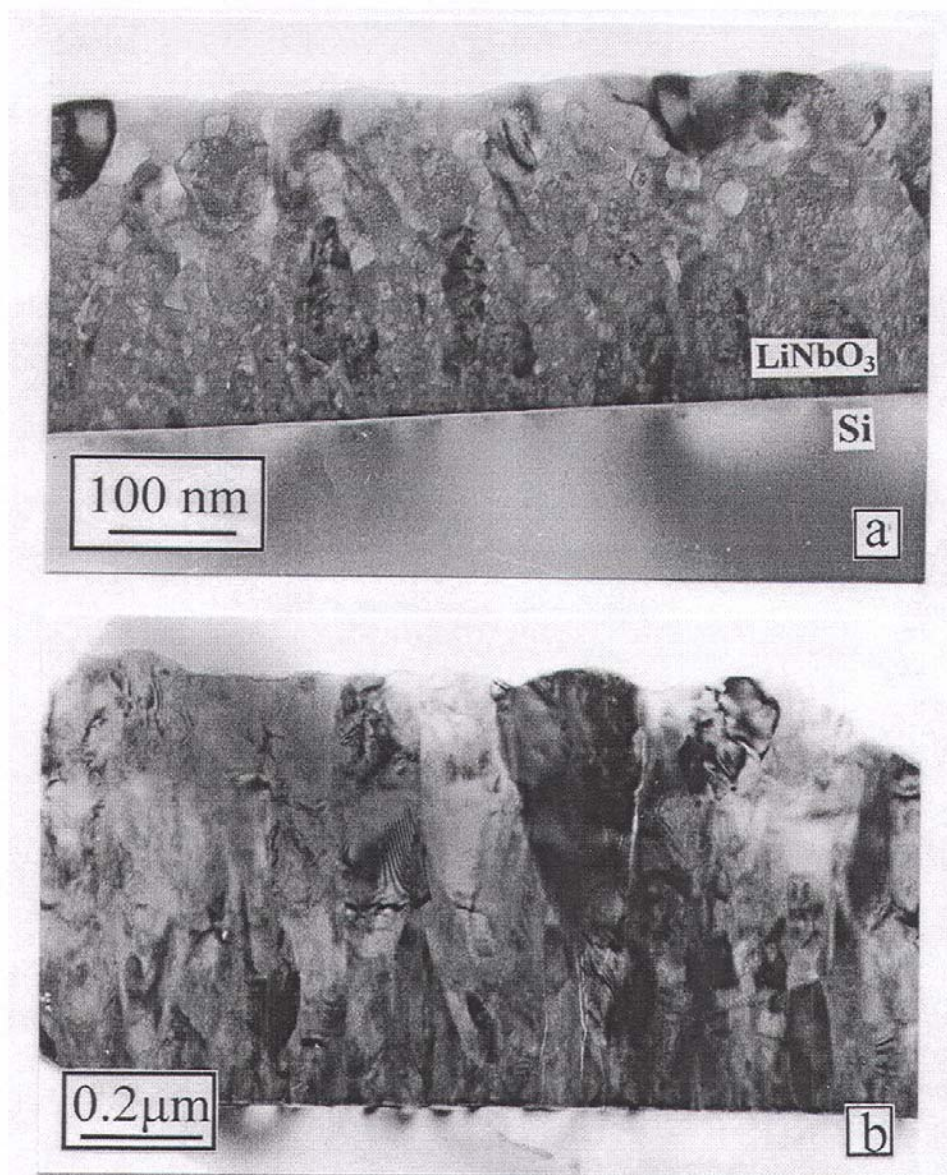


*Fig. 1 Low magnification XTEM images of a LiNbO_3 thin films obtained by pulsed laser deposition
a - as deposited film on Si substrate (500 °C substrate temperature)
b - film deposited on Si at 550 °C and 1h thermal treatment in oxygen atmosphere at 700 °C.*

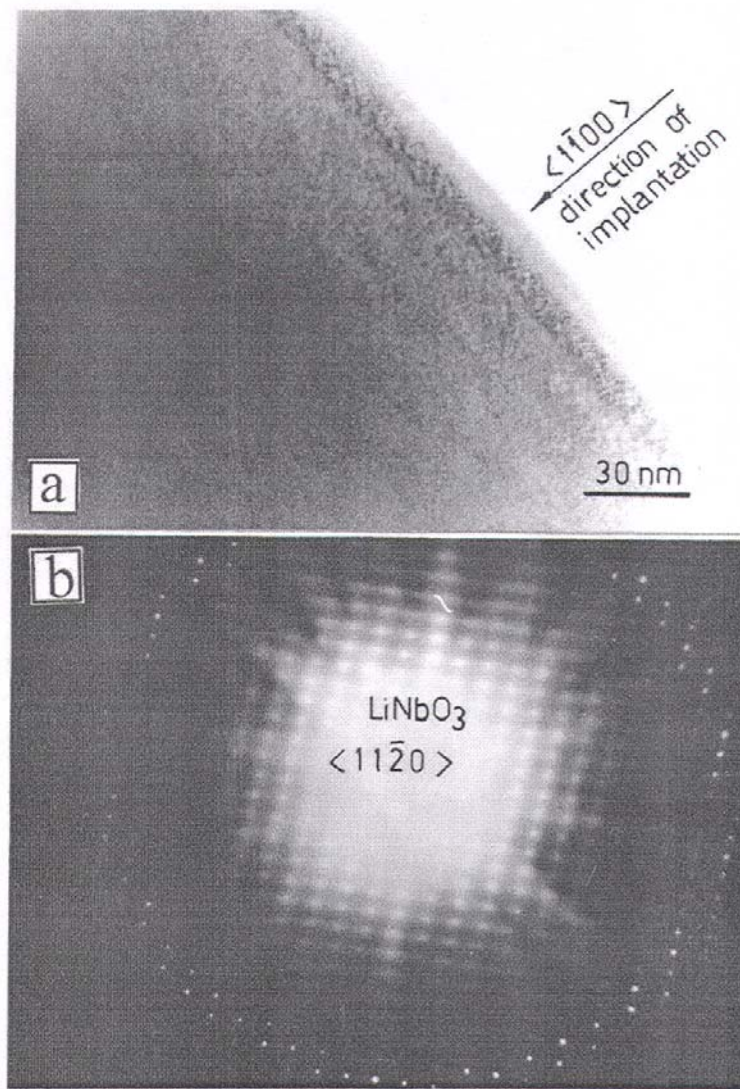


Fig. 2 Low magnification XTEM on the Er implanted edge of a LiNbO₃ wafer (a) oriented in the $[1\bar{1}20]$ zone axis (b).

The EDX spectrum shown in Fig. 3 revealed only traces of Er, because the Er atoms were diffused in a layer of about 100 nm after the thermal treatment.

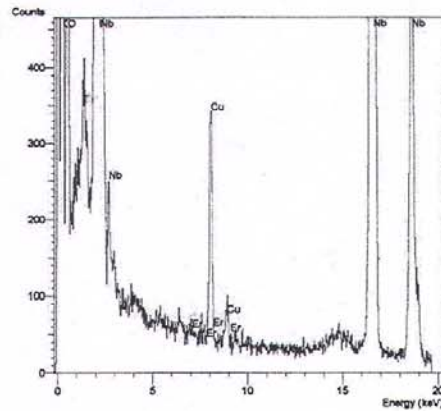


Fig. 3 EDX spectrum from the Er implanted area of the LiNbO_3 sample.

An interesting aspect is the presence of the black band near the surface, which is not a thickness or a Bragg contrast band demonstrated by the corresponding SAED pattern (Fig. 2b) showing the exact zone axis orientation. The origin of the dark band contrast can be explained by observing the high resolution image which shows a nonuniform contrast of the atomic columnar spots (Fig. 4a). Fig. 4 presents the high resolution (HRTEM) images obtained from implanted area after the first minute (Fig. 4a) and after 5 minutes of observations (Fig. 4b) in high resolution mode. The structure of the sample is not stable under the focused electron beam.

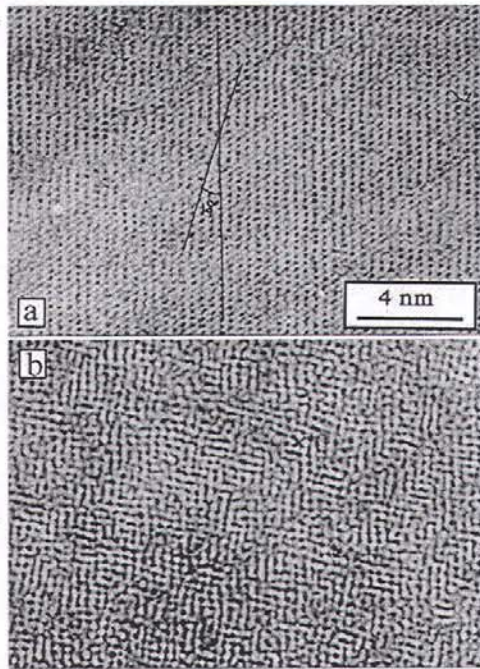


Fig. 4 HRTEM image of the $[1102]$ zone axis of the implanted LiNbO_3 in the first minute of observation (a) and after 5 minutes (b).

The structural modifications induced by the electron irradiation consist mainly in a quasi square organized new phase lattice with nuclei of 2 or 3 nm in size, developed during observation in HRTEM mode. Boundaries between new phase nuclei are quite amorphous with about 1nm thickness. The beginning of the structural transformation is rather fast compared to the late evolution. Images like in Fig. 4a are relatively stable in the microscope. No structural modifications are observed at low beam density in diffraction mode, this suggesting that a threshold value for the electron beam intensity is operating. The new phase formation leads to the appearance of diffused spots in the SAED pattern (Fig. 5b). The extension of these diffused spots in the reciprocal space suggest the presence of cuboidal nanometric structure.

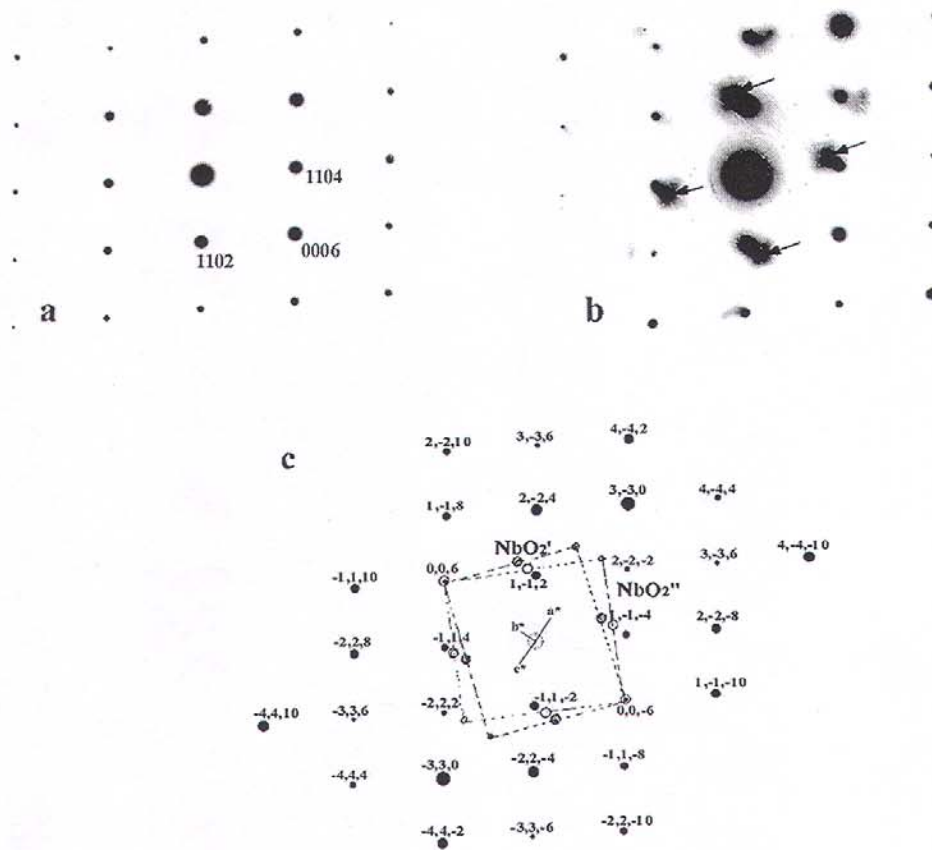


Fig. 5 SAED patterns from the irradiated area. (a) – LiNbO_3 - $[1102]$ zone axis in the first minute of observation, (b) – the same area after 5 minute of high resolution observation showing additional spot, (c) – sketch of the indexing of the electron diffraction pattern.

The disposal of the supplementary spots in the reciprocal space reveals a superposition of several orientations of the new phase nucleus respective to the old niobate lattice. Regarding the electron irradiation damage, like a decomposition of the LiNbO_3 structure, the closed type of known structure which can explain the main features observed in the TEM and SAED images is the simple tetragonal NbO_2 structure. It is also possible that the NbO_2 nuclei formed in the niobate matrix consist in a new, unknown, cubic metastable phase.

We must point out that the decomposition of the LiNbO_3 lattice was not observed in the case of cross section films studies [5] and also not in the case of powder LiNbO_3 samples [10]. Fig. 6 shows a SAED pattern of the pseudo-cubic $[2201]$ zone axis of the LiNbO_3 microcrystals exposed more than 500 second to high current density electron beam. No additional spots are present.

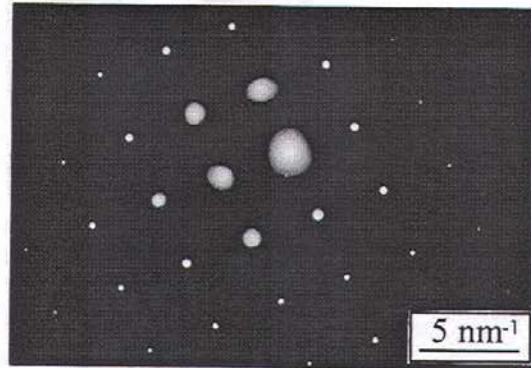


Fig. 6 SAED pattern realized on LiNbO_3 microcrystals obtained by grinding the LiNbO_3 monocrystal wafer in $[2201]$ pseudocubic- orientation. The pattern are recorded after about 500 second TEM observation in focused electron beam.

In Fig. 7 is presented the schemas of the real (a) and the reciprocal (b) space of the LiNbO_3 and the NbO_2 structures. Using these two schemas it is possible to explain the main features present in the SAED pattern of the irradiated LiNbO_3 sample. The indexing of this SAED pattern is shown in Fig. 5c. This analysis shows that the most probable crystallographic relationships in the decomposition of the lithium niobate seems to be $(0006)_{\text{LiNbO}_3} // (111)_{\text{NbO}_2}$ with two different positions of the NbO_2 nucleus aligned parallel to the pseudo-cubic axis of the niobate. Fig. 8 shows a superposition of the real space structure of the LiNbO_3 seen in the $[11\bar{2}0]$ orientation with the two possible orientations of NbO_2 . In this schematics the $[2201]_{\text{LiNbO}_3} // [101]_{\text{NbO}_2}$ alignment was used. The development of the NbO_2 nuclei introduces also a rotation with 16 degrees of the trace of (1102) crystallographic plane of the lithium niobate in the high resolution images (see Fig. 5b).

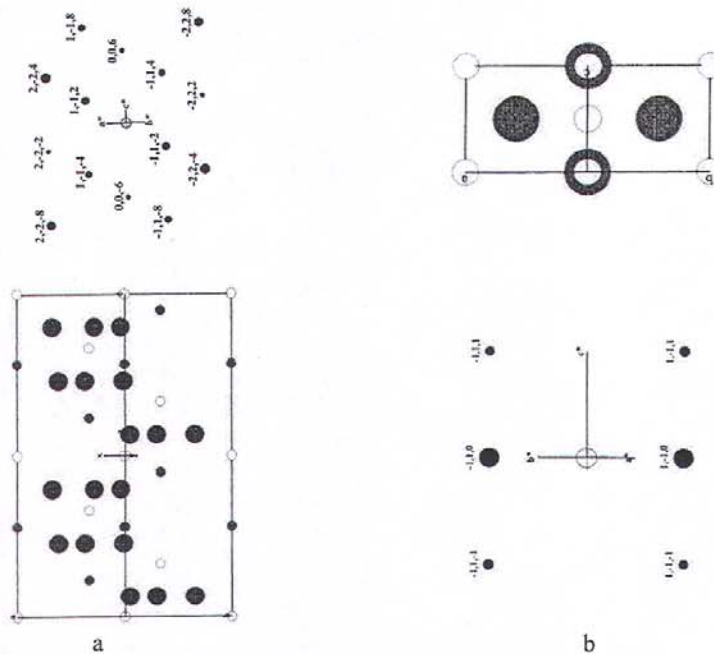


Fig. 7 Images of the real and the reciprocal spaces of LiNbO_3 (a) and NbO_2 (b) structures.

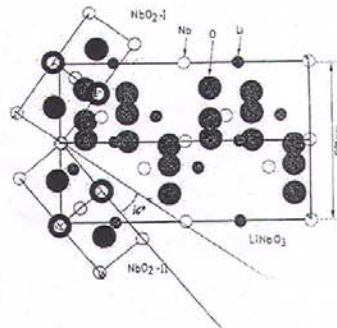


Fig. 8 Sketch of the superposition of the $[11\bar{2}0]$ LiNbO_3 zone axis and the two different position of the $[110]$ NbO_2 aligned parallel to the pseudo-cubic axis of the niobate Schematic of the two different equivalent orientations of the topotactic orientations between the LiNbO_3 matrix and the NbO_2 nuclei.

4. Discussions and conclusions

It is suggested that the ionizing damage induced by electron irradiation of implanted crystal results into the thermally activated decomposition of the non-stoichiometric layer generated by thermal annealing. This decomposition gives rise to the formation of nanodomains of NbO_2 (probably the simple tetragonal phase with $a = 0.484$ nm and $c = 0.303$ nm) in a matrix of Li and O deficient lithium niobate.

These phenomena are not observed or are less pronounced in non implanted LiNbO_3 crystals where the non stoichiometric surface layer does not exist, providing enough defect sites and species for further non-stoichiometric reaction resulting from electron irradiation damage.

From these investigations we have evaluated the values of the beam current density (less than 30 A/cm^2) which can be used for image recording in the first minute of observation in order to obtain images less (or not) affected by the radiation damage. Under such conditions, the contrast of the high resolution lattice images can be interpreted with respect to the structure of the starting material or of the defects correlated with implantation of erbium ions [9].

In the conventional TEM studies on LiNbO_3 samples at low density electron beam, there were not observed any influence due to the electron beam irradiation. The structure of the thin films at high resolution is more stable in the electron beam, but care must be taken in the interpretation of different defects which can appear at nanoscale magnification.

References

- [1] Agullo-Lopez F., Cabrera J., "Point Defects in Lithium Niobate" in "Properties of Lithium Niobate" ed. INSPEC, The Institution of Electrical Engineers, pag. 8, 1989.
- [2] Weis R.S., Gaylord T.K., Appl.Phys. A **37**, 191(1985).
- [3] Afonso C.N., Gonzalo J., Vega F., Dieguez E., Cheang J., Wong C., Ortega C., Siejka J., Amsel G., Appl. Phys. Lett. **66**, 1452(1995).
- [4] See-Hyung Lee, Tae Kwon Song, Noh T.W., Jai-Hyung Lee, Appl. Phys. Lett. **67**, 43(1995).
- [5] Ghica D., Ghica C., Gartner M., Nelea V., Martin C., Cavaleru A., Mihailescu I.N., Applied Surface Science **192**, 133(1999).
- [6] Hobbs L.W., J. Physique C-9, **11-12**, 227(1973).
- [7] Teodorescu V.S., Nistor L.C., Van Landuyt J., Materials Science Forum **239-241**, 671(1997).
- [8] Teodorescu V.S., Blanchin M.G., Proc. EURODIM 98, Radiation Effects & Defects in Solids (in press 1999).
- [9] Teodorescu V.S., Blanchin M.G., Mignotte C., Moretti P., Traverse A. (J. Appl. Phys., submitted).
- [10] Leroux C., Nihoul G., Malovichko G., Grachev V., Boulesteix C., J. Phys. Chem. Solids **59**, 311 (1998).